The importance of accounting for the north Atlantic oscillation when applying observational constraints to European climate projections

Geophysical Research Letters

RESEARCH LETTER
10.1029/2023GL103431

Key Points:

- Variability in the North Atlantic Oscillation (NAO) has contributed to the recent multidecadal trends observed in European climate
- The suite of current comprehensive global models (CMIP6) struggle to reproduce the NAO's contribution to multidecadal trends
- Removing the NAO from both observations and models provides a tighter, unbiased constraint, which can then be applied to model projections

Supporting Information:

Supporting Information may be found in the online version of this article.

Correspondence to:

A. P. Ballinger,
andrew.ballinger@ed.ac.uk

Citation:

Ballinger, A. P., Schurer, A. P., O'Reilly, C. H., & Hegerl, G. C. (2023). The importance of accounting for the North Atlantic Oscillation when applying observational constraints to European climate projections. *Geophysical Research Letters*, *50*, e2023GL103431. https://doi.org/10.1029/2023GL103431

Received 27 FEB 2023
Accepted 27 JUL 2023

The Importance of Accounting for the North Atlantic Oscillation When Applying Observational Constraints to European Climate Projections

Andrew P. Ballinger[1], Andrew P. Schurer[1], Christopher H. O'Reilly[2], and Gabriele C. Hegerl[1]

[1]School of GeoSciences, University of Edinburgh, Edinburgh, UK, [2]Department of Meteorology, University of Reading, Reading, UK

Abstract Variability in the North Atlantic Oscillation (NAO) has contributed to the recent multidecadal trends observed in European climate, especially to trends in winter precipitation over Northern Europe. However, the current generation of coupled climate models struggle to reproduce the NAO's contribution to multidecadal trends, which has important implications for deriving constraints based on the comparison of observed and modeled trends. An observational constraint based on attribution results, both with and without the contribution of variability associated with the NAO, is applied to projections of Northern European precipitation and temperature, and observed NAO variability is shown to lead to a constraint that overestimates future forced changes. Only after removing the NAO variability is the observed climate change consistent with model simulations, and a tighter, unbiased observational constraint based on the forced signal (without the NAO) can be applied to future projections.

Plain Language Summary The observed precipitation and temperature across Northern Europe in winter has been increasing over the past several decades. However, the magnitude of this trend is generally not well reproduced by the latest set of global climate models. A part of the observed increase in precipitation can be related to the variability in the North Atlantic Oscillation (NAO), which is a large-scale pattern of sea level pressure in the North Atlantic region that varies in strength each season and year, and is strongly linked to temperature and precipitation patterns across Europe, particularly in winter. In this study, we show that if the variability related to the NAO is first removed from the precipitation time series, from both the observations and the model simulations, the difference between the long-term observed and modeled trends in precipitation is reduced. Removing the NAO variability also has an impact on the difference in observed and modeled trends in temperature. This has important implications for approaches that use the difference in observations and model simulations as a way of constraining future projections of climate change.

1. Introduction

The North Atlantic Oscillation (NAO) is the leading mode of climate variability over the North Atlantic region, affecting temperature and precipitation from days to seasons and decades (Hurrell et al., 2003). Positive NAO values have been shown to cause anomalously warm temperatures across Northern Europe and Eurasia in winter, accompanied by anomalously wet anomalies in Scandinavia and drier conditions in the Western Mediterranean (Hurrell & Van Loon, 1997; Thompson et al., 2000). The NAO has important relevance to seasonal prediction, with predictability over months to possibly years, although with insufficient amplitude in the initialized predictions (Scaife & Smith, 2018; Smith et al., 2020).

Various studies have shown that multidecadal variations in the NAO yield significant trends in twentieth century European temperature and precipitation, especially in winter (e.g., Deser et al., 2016, 2017; Hurrell, 1995; Iles & Hegerl, 2017). However, the magnitude of observed multidecadal NAO variability in the past is generally not reproduced by current Coupled Model Intercomparison Project (CMIP6; Eyring et al., 2016) models (Blackport & Fyfe, 2022; Eade et al., 2022; O'Reilly et al., 2021; A. P. Schurer et al., 2023). Furthermore, climate model simulations project at most modest forced changes in the NAO in the future (Lee et al., 2021). Here we show that this discrepancy in NAO variability has important implications for deriving observational constraints on projections of European climate.

By estimating the forced component of change from observations, a constraint can be derived and applied to future projections based on the assumption that any relationship between observations and models can be extrapolated into the future. For example, if past forced changes simulated by climate models underestimate the observed changes over the same time period, future projected changes by the same climate models may also underestimate the *true* forced signal in the future. One such approach, hereafter the Allen-Stott-Kettleborough "ASK" method (Allen et al., 2000; Allen & Stott, 2003; Shiogama et al., 2016; Stott & Kettleborough, 2002) has been used for constraining global projections, including for the Intergovernmental Panel on Climate Change (Knutti et al., 2008), and was recently employed in a multi-method study of constrained European climate projections (Brunner et al., 2020). The strength of the ASK method is that it uses well-understood patterns of response to external forcings to determine from observations the magnitude of the response. ASK allows a magnitude of response outside the model range, and also lends itself to estimating the transient and equilibrium climate sensitivity (Frame et al., 2005; A. Schurer et al., 2018; Tokarska et al., 2020).

However, regional climate change is strongly influenced by internal variability. ASK accounts for this, but cannot do so correctly if the climate model decadal circulation variability is smaller than observed, as appears to be the case for the NAO (e.g., O'Reilly et al., 2021; A. P. Schurer et al., 2023). This study demonstrates that NAO variability can strongly influence observational constraints on European climate, particularly in winter. In order to evaluate its effect, we remove the influence of the NAO from the time series of regional mean precipitation and temperature change by linear regression and then apply the ASK method. Here we use two different sets of fingerprints and samples of variability, one with and one without the NAO. Focusing on winter precipitation and temperature over Northern Europe, we show the NAO has a marked influence on the magnitude (and uncertainty estimate) of the derived observational constraints, with important ramifications for their application to future climate projections. Similar concerns may arise for observational constraints in other regions influenced by the NAO, such as Mediterranean temperature and precipitation (not shown).

2. Data and Methods

2.1. Observations and Climate Model Simulations

Gridded observations of European precipitation and surface air temperature over land were retrieved from the E-OBS v19.0e data set (Cornes et al., 2018; Haylock et al., 2008), with monthly values computed from the daily data (1950–2019). The observed NAO was computed from gridded sea level pressure (SLP) (see Section 2.2) retrieved from HADSLP2 (Allan & Ansell, 2006). The study analyzes CMIP6 global climate model simulations run with historical forcings (1850–2014). The common period from 1950 to 2014 was used for analysis of monthly precipitation (a total of 163 ensemble members from 41 CMIP6 models) and surface air temperature (178 ensemble members, 49 models), see Table S1 of Supporting Information S1. To facilitate comparison with observations, the monthly precipitation and temperature fields (for each of the model ensemble members) were spatially regridded to a regular 2.5° × 2.5° latitude–longitude grid, and masked to retain only the gridboxes over land, matching the E-OBS data availability. In order to explore the impact on future projections, historical simulations were extended with CMIP6 Scenario-MIP Shared Socioeconomic Pathway (SSP; Gidden et al., 2019) simulations (2015–2100), thus only the subset of model ensemble members common to both the historical and scenario experiments have been used for the observational constraint (see Table S1 in Supporting Information S1).

2.2. Removing the NAO Variability

For this study, we characterize the NAO variability by the first Empirical Orthogonal Function (EOF) of SLP over the North Atlantic sector (20°–90°N; 90°W–40°E). The EOF and first principal component time series is computed for each month's (1950–2014) anomalous SLP, separately, in order to construct a monthly time series of the NAO. The spatio-temporal European precipitation is then regressed against the NAO time series, separately for each month, in order to compute the component of observed precipitation associated with the NAO, accounting for seasonal variations in the response. This is repeated for the observed temperature field, identifying the component of European temperature anomalies associated with NAO variability. The individual NAO time series for each of the CMIP6 models is computed from its own SLP field, followed by a regression of each model ensemble member's European temperature and precipitation fields on its own NAO time series (1950–2014, month by month). The resulting multi-model mean EOF and regression patterns are similar to the

corresponding observed patterns (Figures S1 and S2 in Supporting Information S1; see also Deser et al., 2017; Iles & Hegerl, 2017). The residual spatio-temporal fields provide an estimate of the monthly European precipitation and temperature anomalies after the component linearly related to the NAO variability has been removed. We acknowledge that this approach is limited to removing the linear response and will miss any nonlinear aspects of the NAO's influence on European climate. However, Iles and Hegerl (2017) found that aggregated NAO temperature trend responses in models (allowing for nonlinearity) were similar to estimates using a linear assumption; and results from Deser et al. (2017) suggests this is also broadly the case for precipitation.

2.3. Allen-Stott-Kettleborough (ASK) Method

The ASK method (Allen & Stott, 2003; Allen et al., 2000; Stott & Kettleborough, 2002) assumes that the true observed climate response (y_{obs}) to historical forcing(s) is a linear combination of one or more (n) individual forcing fingerprints (X_j). The fingerprints are scaled to best fit the observed change by their respective scaling factors (β_j), accounting for noise/uncertainty in both the observations (ε_{obs}), and in the modeled response to each of the forcings (ε_j):

$$y_{\text{obs}} = \sum_{j=1}^{n} \beta_j (X_j - \varepsilon_j) + \varepsilon_{\text{obs}} \tag{1}$$

When applied to global-scale temperature, ASK estimates the contribution from the greenhouse gas fingerprint against that of other forcings, and then uses this to constrain future warming. However, the climate change signal for winter precipitation and temperature in a small region is expected to have a much lower signal-to-noise ratio. We therefore use fingerprints of the total forcing response. This approach is supported by the finding that anthropogenic forcing is dominant against natural forcing (see Gillett et al., 2021), and that anthropogenic forcing provides reasonable future constraints (Tokarska et al., 2020).

Thus, we employ a one-signal *all-forcing* application of Equation 1, $y_{\text{obs}} = \beta_{\text{All}} X_{\text{Hist}} + \varepsilon$, constructing the model fingerprint (X_{Hist}) by taking an unweighted average of the individual historically forced model-ensemble means from the CMIP6 historical simulations, spatially averaged over the region of interest. This results in a time-dependent fingerprint of the regional forced change. The scaling factor is estimated $\left(\hat{\beta}_{\text{All}}\right)$ by computing a total least squares (TLS) regression of the observed time series on the model fingerprint. We assume that the internal variability of the multi-model mean is reduced by a factor of $\sqrt{\sum_{k=1}^{N} m_k^2}$ due to ensemble averaging, where m_k is the number of ensemble members belonging to each of the N models. Random samples from the pre-industrial control simulations are added to both the noise-reduced model fingerprints and observations, recomputing the TLS regression (10,000 times) in order to build a distribution of scaling factors and estimate their 5th–95th percentile range. This results in a range of model response that is consistent with the observations given internal variability. This approach is applied to both raw observations, and forced and control simulations; and to those from which the NAO influence has been removed from all components.

When applied as an observational constraint on the forced component of future climate model projections (following Kettleborough et al., 2007), the best estimate of the scaling factor $\left(\hat{\beta}_{\text{All}}\right)$, along with the 5th–95th percentile range, is multiplied by the CMIP6 multi-model mean anomaly that was used as a fingerprint. This provides a constrained estimate of the range of the forced response in future model projections, with anomalies in reference to a 1950–2014 baseline, the period over which the scaling factor is also calculated. Similar implementations of the ASK approach have recently been applied to constrain future projections of temperature and precipitation across European regions (Brunner et al., 2020; Hegerl et al., 2021), with a particular focus on summer temperature. The results will focus on Northern European precipitation and temperature, particularly in winter, given the well-known influence of the NAO.

3. Results

3.1. The NAO's Contribution to Variability and Trends

The contribution of NAO variability to recent multidecadal trends in Northern European winter climate is illustrated for both the observations (Figures 1a–1d) and model simulations (Figures 1e and 1f). As expected, removing the influence of the NAO reduces the interannual variability of the observed time series of precipitation

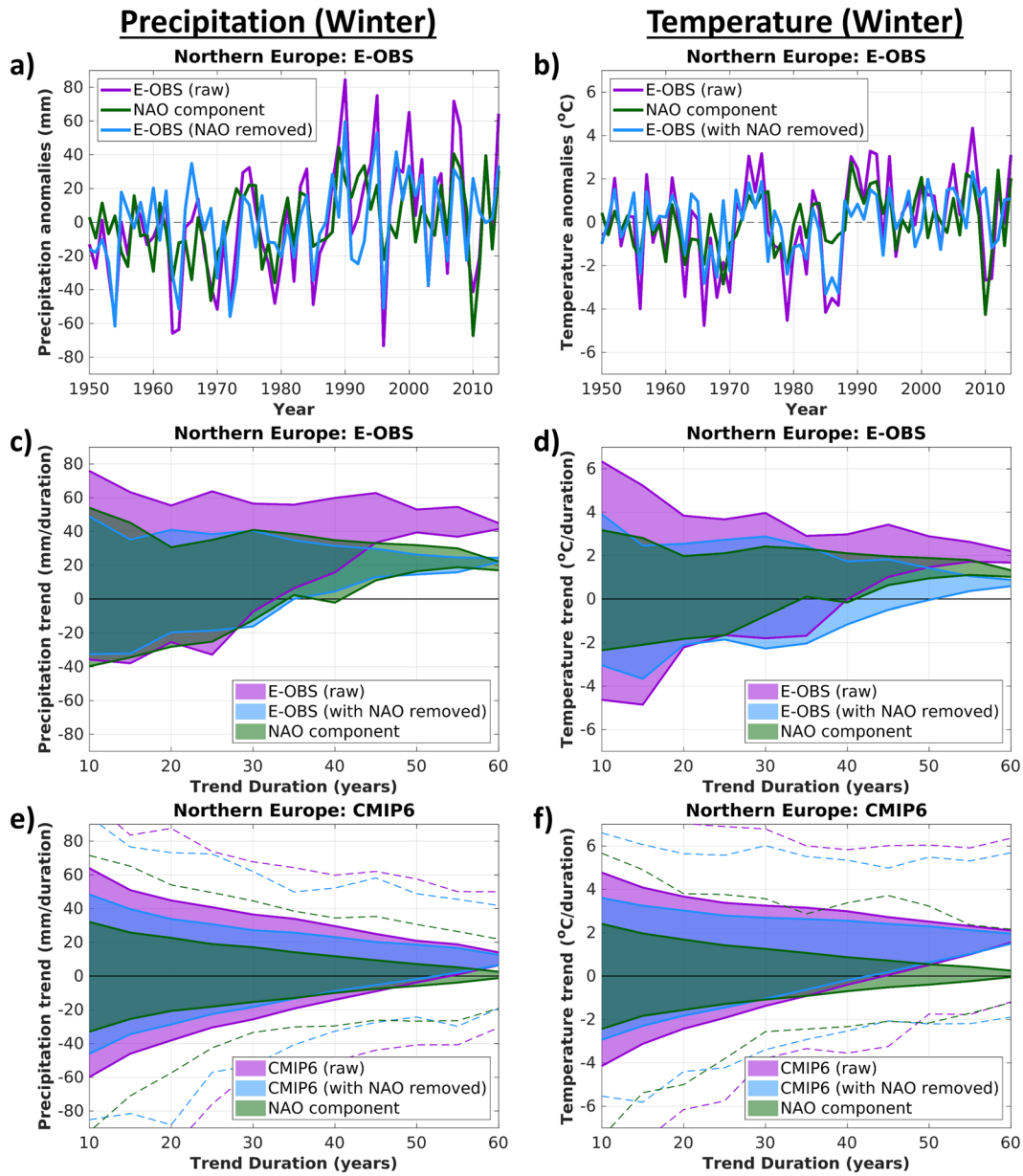

Figure 1. (a, c, and e) Time series (1950–2014) and associated trend distributions of winter (DJF) precipitation and (b, d, and f) temperature anomalies for Northern Europe, computed from (a–d) E-OBS observations and (e–f) the CMIP6 suite of historical simulations. Purple colors denote the raw time series (and trends), green shows the component associated with the North Atlantic Oscillation (NAO), and blue shows the residual after the NAO has been removed. Shaded regions show the range of all linear trends (of 10- to 60-year duration, along the *x*-axis) sampled over the 1950–2014 period, (c and d) spanning the minimum to maximum observed trends, and (e and f) spanning the weighted CMIP6 multi-model mean minimum to maximum trends from the individual ensemble member trend distributions, with the dashed lines depicting the minimum and maximum trends from *any* of the individual simulations. Units show the change in (c and e) total winter precipitation or (d and f) temperature over the trend duration (in years).

(Figure 1a) and temperature (Figure 1b). The corresponding panels below (Figures 1c and 1d) show the distributions of multi-year linear trends, with the distribution for a trend duration of *n* years formed from all possible *n*-yr periods within 1950–2014. The 30-year trends in winter precipitation (i.e., 36 trends throughout the 1950–2014 period) range from a minimum of a ∼5 mm decrease to a maximum of ∼60 mm increase, with the majority of 30-year trends showing an increase of ∼20–40 mm (Figure 1c). The estimated contribution to the trends over the same 1950–2014 period that is associated with the observed variability of the NAO (green shading) indicates

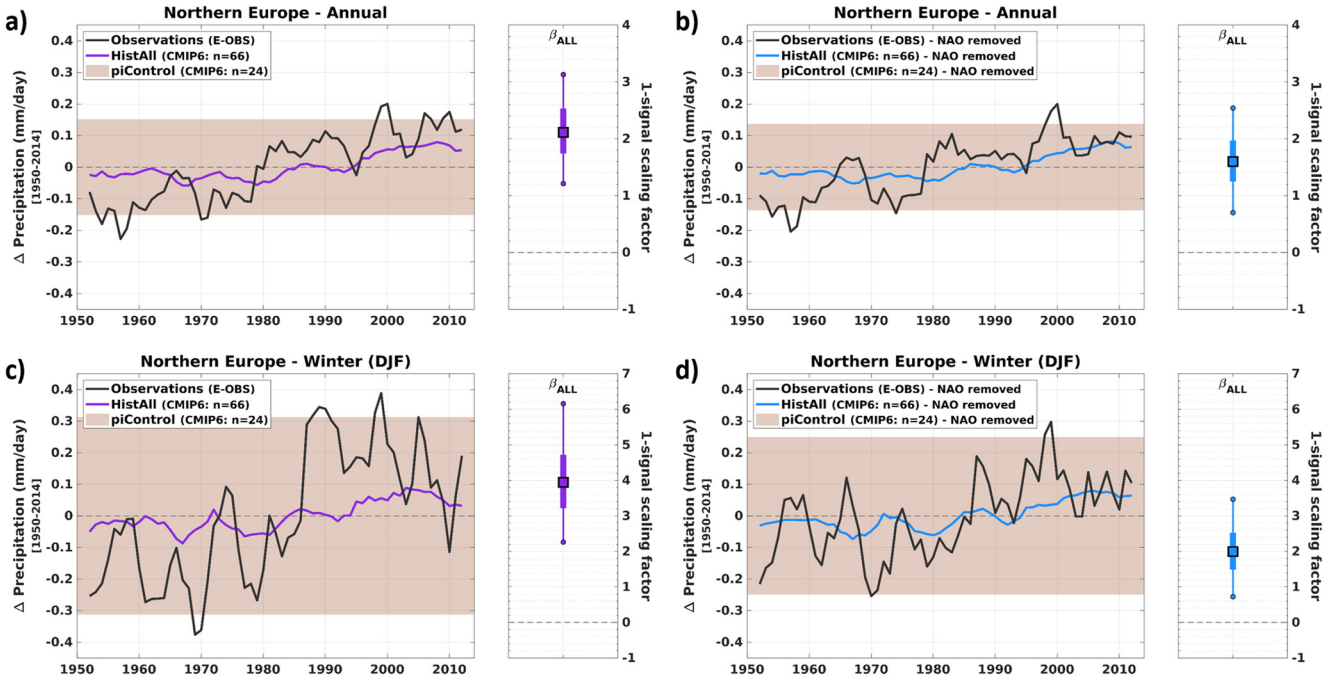

Figure 2. (a and c) Time series of Northern European precipitation anomalies (relative to 1950–2014) from observations (E-OBS v19, black lines) and CMIP6 historical simulations (all forcings, colored lines, displaying the multi-model mean of ensemble means (24 models, 66 total ensemble members)), showing the original time series, and (b and d) the time series with the North Atlantic Oscillation removed, (a and b) for annual, and (c and d) winter DJF accumulated precipitation. Time series have been smoothed with a 5-year running mean, and the shaded region denotes the mean variability (±1 standard deviation) of the associated pre-industrial control simulations. The 1-signal scaling factor ($\hat{\beta}_{\mathrm{All}}$, shown to the right of each panel) was derived from a total least squares regression of the CMIP6 model fingerprint on the observations, indicating to what extent the multi-model mean fingerprint needs to be scaled to best match observations (central square marker), along with the scaling range (5th–95th percentile) that is consistent with observations.

that for trends longer than ~35–40 years the NAO has contributed positively to observed annual precipitation trends, irrespective of the starting year of the trend (see also Blackport & Fyfe, 2022). An increase of ~20 mm in Northern European winter precipitation, and an increase of ~1°C in winter temperature, can be attributed to the influence of the NAO over a period of ~40–60 years. Once the impact of NAO variability has been regressed out of the raw time series, the residual trends over the same period are markedly reduced. In fact, the residual ~40–60-year trends are less than (for temperature), or comparable to (for precipitation) the magnitude of the trends owing to variability in the NAO alone.

In contrast to the impact of removing the NAO on observed trends, the primary impact of removing the NAO from simulations is to reduce the variability and thus narrow the range of residual trends modeled over the historical period (Figures 1e and 1f). While a multi-model mean range of ~±20 mm is estimated for the component of all 30-year winter precipitation trends associated with the NAO (e.g., in Figure 1e), there are rare individual ensemble members that have NAO trends that are as much as twice this magnitude. Nevertheless, the long-term increasing trend in winter precipitation is substantially weaker (a factor of 3–4) in the multi-model mean than observed, consistent with the models having smaller trends associated with the NAO, and smaller multidecadal NAO variability,as discussed above. Removing the NAO from long-term precipitation trends (blue shading, Figures 1c and 1e) reduces the difference between simulations and observed, whereas for temperature (Figures 1d and 1f) the difference increases.

3.2. The NAO's Impact on the Regional Constraint

The $\hat{\beta}_{\mathrm{All}}$ scaling factors derived for Northern European precipitation are shown in Figure 2, computed using the annual (Figures 2a and 2b) and winter (Figures 2c and 2d) time series, retaining the NAO variability (Figures 2a and 2c), and with the NAO removed (Figures 2b and 2d; note the reduced variability in the observed time series and the control simulations). The scaling factors show that there has been a detectable change in Northern European annual and winter precipitation $\left(\hat{\beta}_{\mathrm{All}} > 0\right)$. However, unless the NAO is removed, the magnitude of the

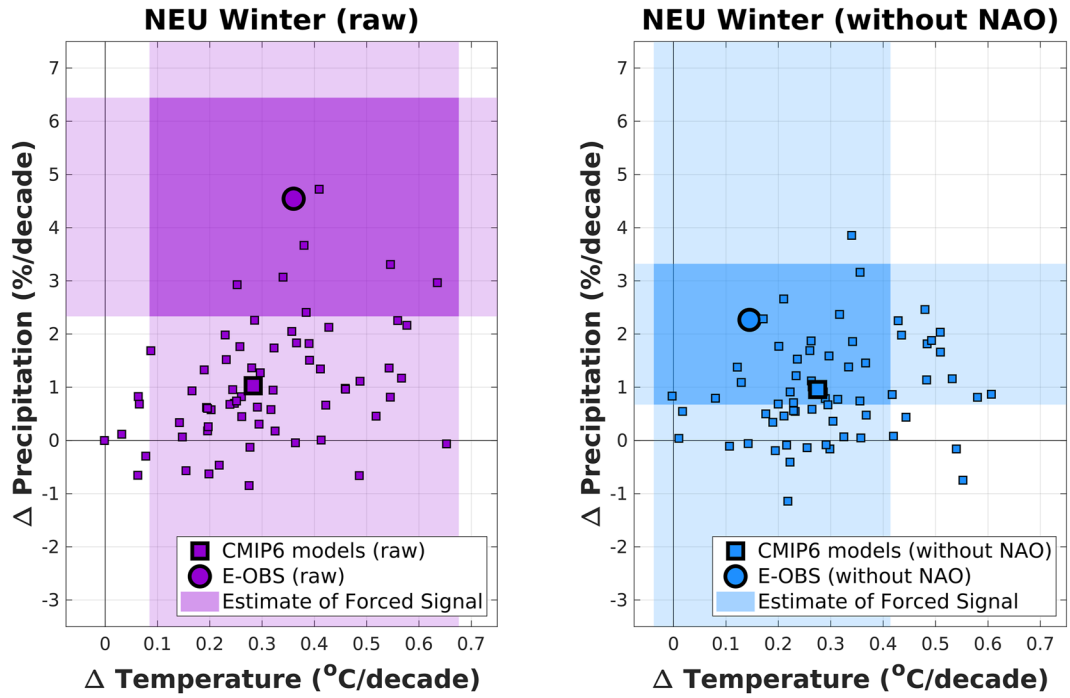

Figure 3. The change in mean surface air temperature (horizontal axis; °C decade^{-1}) and precipitation (vertical axis; % decade^{-1}) between the periods 1950–1969 to 1995–2014, for Northern European (NEU) winter (DJF) over land. Square markers show the individual CMIP6 model ensemble members ($n = 66$), and the multi-model mean (large square). Circle markers show the observations (E-OBS, v19). Purple colors (left panel) indicate the analysis of the raw time series, while blue colors (right panel) show the analysis after regressing out the North Atlantic Oscillation. The shaded regions display the estimated range (5th–95th percentile) of the forced signal, computed by multiplying the CMIP6 multi-model mean change by the derived scaling factor $(\hat{\beta}_{\mathrm{All}})$, separately for temperature and precipitation.

model fingerprint is not consistent with observations (i.e., the range in $\hat{\beta}_{\mathrm{All}}$ does not include unity), and needs to be scaled by a factor of 1.4–3.8 in annual data (Figure 2a), and even more in the winter (2.2–6.0; Figure 2c), to reproduce observed changes. After removing the NAO (Figures 2b and 2d) the best estimate scaling factors are reduced, especially in winter, and the constraint also tightens (i.e., the spread in scaling factors narrows) due to the increased signal-to-noise in the modeled response once the NAO is removed. The scaling factors for temperature are shown in Figure S3 of Supporting Information S1, and similarly indicate a reduction and tightening of the constraint, especially in winter, once the NAO is removed.

Past changes in Northern European winter temperature and precipitation are shown together in Figure 3, with individual climate model simulations from CMIP6 historical model ensemble members (small squares; large square for multi-model mean) compared to observed changes (circles). The change displayed is between 1950–1969 and 1995–2014, but results are similar if choosing linear trends or slightly different periods (not shown). The left panel shows the changes with NAO variability retained, with an observed warming of ~0.35°C per decade, and wettening of ~4.5% per decade. While there is a spread in the CMIP6 model simulations, with warming rates between ~0–0.65°C per decade, for precipitation all but one of the model ensemble simulations have lower trends than observed, including some showing a slight drying between the periods (~−0.9%–4.8% per decade). The multi-model mean change in winter temperature is slightly less than the observed change (~0.28°C per decade), while for precipitation the mean change (~1% per decade) is significantly lower than observed, consistent with the earlier comparison of trend distributions and scaling factors. The purple shaded region depicts the externally forced change in the observations, as estimated from the range of scaling factors (5th–95th percentile spread of $\hat{\beta}_{\mathrm{All}}$, recalling Figure 2c and Figure S3c in Supporting Information S1) multiplied by the historical change in the multi-model mean for temperature and precipitation separately. Only a small fraction of individual simulations (~10%) show a past change that is consistent with the observational constraint in both variables and indicates that there is only a modest chance of internal variability or model uncertainty explaining the discrepancy. Thus, without removing the NAO the multi-model mean is inconsistent with the observed precipitation change. CMIP6

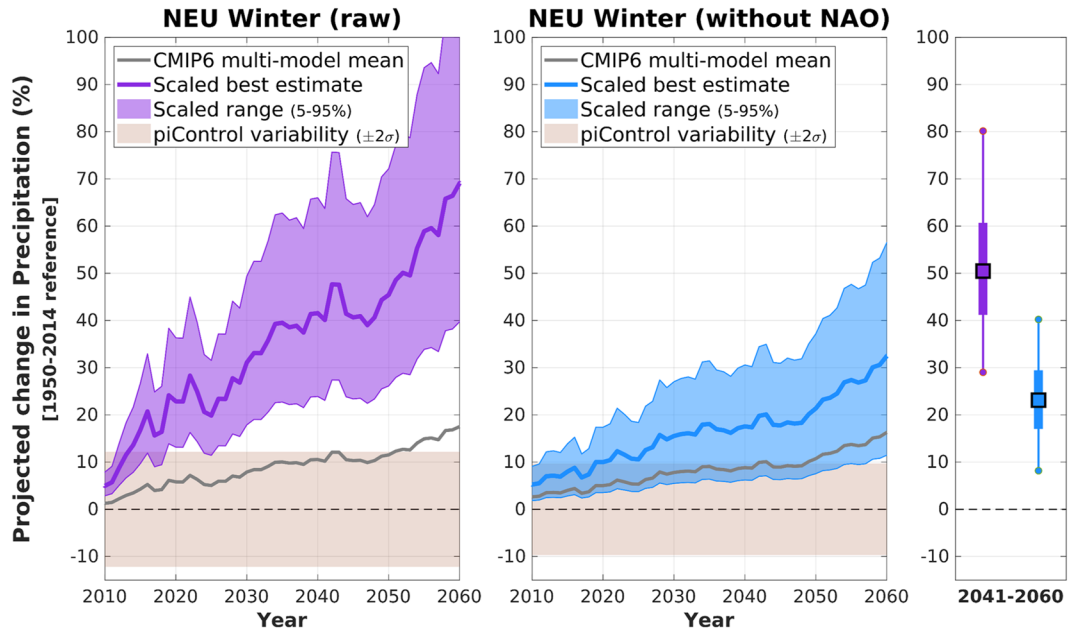

Figure 4. The impact of applying an observational constraint, before and after regressing out the associated North Atlantic Oscillation (NAO) variability. The left panel (purple) shows the constrained projection using the Northern European winter (DJF) raw precipitation, and the middle panel (blue) shows the constrained projection after first regressing out the component of precipitation that is associated with the NAO (from both models and observations). The gray lines show the CMIP6 multi-model mean of ensemble means (66 total simulations from 24 models, forced with historical emissions and the future SSP5-85 scenario from 2015), shown as a percentage change in precipitation relative to a 1950–2014 baseline, with a 5-year running mean. The colored lines show the multi-model mean scaled by the best estimate (and 5th–95th percentile range shaded region) of the scaling factor $\left(\hat{\beta}_{\mathrm{All}}\right)$ required for the historical simulations to be consistent with observed winter precipitation. The mean variability of the 24 pre-industrial control simulations is also plotted. The right panel compares the 20-year mean change (2041–2060) in the constrained projections (best estimate, and 5th–95th percentile range).

simulated changes in winter precipitation are unlikely to be consistent with the estimates of the forced change, even when accounting for model uncertainty and internal variability.

Once the NAO has been removed from the historical time series (Figure 3, right panel), the observed wintertime temperature and precipitation change are each reduced by ∼50%. There is also a slight tightening in the spread of individual model ensemble members while the multi-model mean remains relatively unchanged. Compared to the constraint including the NAO, there is a clear shift in the estimate of the forced component (blue shaded region), and a narrowing of the uncertainty range. The observed increase in Northern Europe winter precipitation that is attributed to anthropogenic forcing reduces from ∼2.3%–6.4% to ∼0.8%–3.2% (relative to climatology, per decade), with more than half of the ensemble members now within this observationally constrained range. The uncertainty range for the forced component of precipitation change narrows and the wintertime past wettening change remains detectable. There is also a reduction in the forced component of winter warming without the NAO, from ∼0.09–0.68°C to ∼-0.03–0.41°C per decade. Thus a forced signal of winter warming is no longer detectable at the $p > 0.05$ level (one-sided tail, note the scaling factor in Figure S3d of Supporting Information S1). Once the NAO variability is removed, several CMIP6 model members show stronger warming than the forced estimate range. While internal variability can help to explain individual simulations having trends outside of the forced range, the presence of these higher-warming models is also consistent with various analyses showing some of the CMIP6 models have a higher climate sensitivity (Forster et al., 2021). The question remains to what extent the observed NAO evolution may have been influenced by external forcing in a way not captured by the CMIP6 ensemble (Smith et al., 2020).

3.3. The NAO's Impact on the Future Constraint

The results presented here also have implications for constraints on future projections, particularly for regional climate change as illustrated in Figure 4. For this example, winter precipitation from the CMIP6 high-emissions

scenario (SSP5-85) was used as the raw future projection time series, extending the historical simulations previously analyzed. Note that the increasing trend in NEU winter rainfall is only projected to emerge from the variability in the pre-industrial control simulations ($\pm 2\sigma$) during the 2050s (Figure 4, left panel). The constrained projection (thick purple line and shading) is computed by multiplying the raw CMIP6 multi-model mean anomaly time series with the best estimate and 5th–95th percentile spread of $\hat{\beta}_{\mathrm{All}}$ (Figure 2c). The large scaling factor has a marked impact on the future projection of NEU winter precipitation, both in terms of the magnitude of trend, and in anticipating an earlier emergence of the forced change in precipitation beyond the pre-industrial climatology. For the 20-year period centered on 2050, for example, (Figure 4, right panel), an increase in the forced component of winter precipitation of ∼30%–80% is projected. Note that the constraint reflects forcing only, and estimated future changes would need to also account for natural (and other) forcings and internal variability.

Figure 4 (middle panel) illustrates the impact of accounting for the NAO on observational constraints to future projections. The trend in the CMIP6 multi-model mean of precipitation once the NAO has been removed is very similar (thin gray lines) to the raw simulations, thus there is little indication of a forced trend in the future NAO within the CMIP6 model projections (see also the historical multi-model mean changes in Figure 3). However, as shown in the previous section, the $\hat{\beta}_{\mathrm{All}}$ scaling factor is reduced substantially after removing the NAO, and thus when applied as an observational constraint on the CMIP6 projection produces a markedly different estimate of the forced change in future NEU winter precipitation. The magnitude of the forced component of future change over the 2041–2060 period is significantly reduced after removing the NAO (more than halving, from a ∼50% to ∼22% increase), and the uncertainty in the forced component narrows. Note that we only consider the forced component of the change, and are neglecting forced changes in the NAO, which are an additional source of uncertainty in estimates of future climate projections beyond the scope of the current study.

4. Summary

The NAO provides a clear example of a large-scale mode of climate variability that can have non-negligible impacts on the detection and attribution of forced trends in observations, as exemplified by its influence on Northern European climate. Past variability in the NAO has contributed to the recent multidecadal trends in winter temperature and precipitation over Northern Europe. The suite of current comprehensive global models underestimate the NAO's multidecadal variability and do not reproduce its contribution to multidecadal trends. The influence of the NAO can distort the estimate of the magnitude of past forced changes, with important ramifications for the application of observation-based constraints on future model projections, and can lead to an overestimate of future changes in Northern European winter precipitation, which could have important implications for adaptation planning decisions. If the NAO is removed before deriving the constraint, the estimated magnitude of the forced signal is lower and the uncertainty range is smaller.

For both detection and attribution, and in order to estimate an observational constraint based on the externally-forced signal, we suggest assessing and, if necessary, removing the influence from major modes of internal variability, particularly if these show poorly understood trends. This will reduce the potential that these modes bias the estimated magnitude of past forced changes, and also helps narrow the uncertainty. Various storylines describing the future progression of large-scale variability could then be superimposed on the forced-only estimate, allowing consideration of an unforced or forced evolution of this variability.

Data Availability Statement

The E-OBS gridded dataset (Cornes et al., 2018) from the Copernicus Climate Change Service is available at https://surfobs.climate.copernicus.eu/dataaccess/access_eobs.php. The HadSLP2 gridded dataset (Allan & Ansell, 2006) is available from the Met Office Hadley Centre at https://www.metoffice.gov.uk/hadobs/hadslp2/data/download.html. The CMIP6 multi-model ensemble dataset (Eyring et al., 2016) is available through the Earth System Grid Federation (ESGF; Cinquini et al., 2014) at https://esgf-node.llnl.gov/search/cmip6/.

Acknowledgments
AB, GH, and COR were supported by the European Climate Prediction (EUCP) project funded by the European Commission's Horizon 2020 programme (Grant Agreement number 776613). AB, GH, and AS were supported by the Global Surface Air Temperature (GloSAT) project funded by the National Environment Research Council (NE/S015698/1). In addition, AS was funded by a University of Edinburgh Chancellor's Fellowship and COR was funded by a Royal Society University Research Fellowship. The authors thank EUCP project partners for their support and discussion, particularly Antje Weisheimer.

References

Allan, R., & Ansell, T. (2006). A new globally complete monthly historical gridded mean sea level pressure dataset (HadSLP2): 1850–2004. *Journal of Climate*, *19*(22), 5816–5842. https://doi.org/10.1175/JCLI3937.1

Allen, M. R., & Stott, P. A. (2003). Estimating signal amplitudes in optimal fingerprinting, Part I: Theory. *Climate Dynamics*, *21*(5–6), 477–491. https://doi.org/10.1007/s00382-003-0313-9

Allen, M. R., Stott, P. A., Mitchell, J. F. B., Schnur, R., & Delworth, T. L. (2000). Quantifying the uncertainty in forecasts of anthropogenic climate change. *Nature*, *407*(6804), 617–620. https://doi.org/10.1038/35036559

Blackport, R., & Fyfe, J. C. (2022). Climate models fail to capture strengthening wintertime North Atlantic jet and impacts on Europe. *Science Advances*, *8*(45), eabn3112. https://doi.org/10.1126/sciadv.abn3112

Brunner, L., McSweeney, C., Ballinger, A. P., Befort, D. J., Benassi, M., Booth, B., et al. (2020). Comparing methods to constrain future European climate projections using a consistent framework. *Journal of Climate*, *33*(20), 8671–8692. https://doi.org/10.1175/JCLI-D-19-0953.1

Cinquini, L., Crichton, D., Mattmann, C., Harney, J., Shipman, G., Wang, F., et al. (2014). The Earth System Grid Federation: An open infrastructure for access to distributed geospatial data. *Future Generation Computer Systems*, *36*, 400–417. https://doi.org/10.1016/j.future.2013.07.002

Cornes, R. C., van der Schrier, G., van den Besselaar, E. J. M., & Jones, P. D. (2018). An ensemble version of the E-OBS temperature and precipitation data sets. *Journal of Geophysical Research: Atmospheres*, *123*(17), 9391–9409. https://doi.org/10.1029/2017JD028200

Deser, C., Hurrell, J., & Phillips, A. (2017). The role of the North Atlantic Oscillation in European climate projections. *Climate Dynamics*, *49*(9/10), 3141–3157. https://doi.org/10.1007/s00382-016-3502-z

Deser, C., Terray, L., & Phillips, A. S. (2016). Forced and internal components of winter air temperature trends over North America during the past 50 years: Mechanisms and implications. *Journal of Climate*, *29*(6), 2237–2258. https://doi.org/10.1175/JCLI-D-15-0304.1

Eade, R., Stephenson, D. B., Scaife, A. A., & Smith, D. M. (2022). Quantifying the rarity of extreme multi-decadal trends: How unusual was the late twentieth century trend in the North Atlantic Oscillation? *Climate Dynamics*, *58*(5), 1555–1568. https://doi.org/10.1007/s00382-021-05978-4

Eyring, V., Bony, S., Meehl, G. A., Senior, C. A., Stevens, B., Stouffer, R. J., & Taylor, K. E. (2016). Overview of the Coupled Model Intercomparison Project Phase 6 (CMIP6) experimental design and organization. *Geoscientific Model Development*, *9*(5), 1937–1958. https://doi.org/10.5194/gmd-9-1937-2016

Forster, P., Storelvmo, T., Armour, K., Collins, W., Dufresne, J.-L., Frame, D., et al. (2021). The Earth's energy budget, climate feedbacks, and climate sensitivity. In V. Masson-Delmotte, P. Zhai, A. Pirani, S. L. Connors, C. Péan, S. Berger, et al. (Eds.), *Climate Change 2021: The Physical Science Basis. Contribution of Working Group I to the Sixth Assessment Report of the Intergovernmental Panel on Climate Change* (pp. 923–1054). Cambridge University Press. https://doi.org/10.1017/9781009157896.009

Frame, D. J., Booth, B. B. B., Kettleborough, J. A., Stainforth, D. A., Gregory, J. M., Collins, M., & Allen, M. R. (2005). Constraining climate forecasts: The role of prior assumptions. *Geophysical Research Letters*, *32*(9), L09702. https://doi.org/10.1029/2004GL022241

Gidden, M. J., Riahi, K., Smith, S. J., Fujimori, S., Luderer, G., Kriegler, E., et al. (2019). Global emissions pathways under different socioeconomic scenarios for use in CMIP6: A dataset of harmonized emissions trajectories through the end of the century. *Geoscientific Model Development*, *12*(4), 1443–1475. https://doi.org/10.5194/gmd-12-1443-2019

Gillett, N. P., Kirchmeier-Young, M., Ribes, A., Shiogama, H., Hegerl, G. C., Knutti, R., et al. (2021). Constraining human contributions to observed warming since the pre-industrial period. *Nature Climate Change*, *11*(3), 207–212. https://doi.org/10.1038/s41558-020-00965-9

Haylock, M. R., Hofstra, N., Klein Tank, A. M. G., Klok, E. J., Jones, P. D., & New, M. (2008). A European daily high-resolution gridded data set of surface temperature and precipitation for 1950–2006. *Journal of Geophysical Research*, *113*(D20), D20119. https://doi.org/10.1029/2008JD010201

Hegerl, G. C., Ballinger, A. P., Booth, B. B. B., Borchert, L. F., Brunner, L., Donat, M. G., et al. (2021). Toward consistent observational constraints in climate predictions and projections. *Frontiers in Climate*, *3*, 678109. https://doi.org/10.3389/fclim.2021.678109

Hurrell, J. W. (1995). Decadal trends in the North Atlantic Oscillation: Regional temperatures and precipitation. *Science*, *269*(5224), 676–679. https://doi.org/10.1126/science.269.5224.676

Hurrell, J. W., Kushnir, Y., Ottersen, G., & Visbeck, M. (2003). An Overview of the North Atlantic Oscillation. In *The North Atlantic Oscillation: Climatic Significance and Environmental Impact* (pp. 1–35). American Geophysical Union (AGU). https://doi.org/10.1029/134GM01

Hurrell, J. W., & Van Loon, H. (1997). Decadal variations in climate associated with the North Atlantic Oscillation. In H. F. Diaz, M. Beniston, & R. S. Bradley (Eds.), *Climatic Change at High Elevation Sites* (pp. 69–94). Springer Netherlands. https://doi.org/10.1007/978-94-015-8905-5_4

Iles, C., & Hegerl, G. (2017). Role of the North Atlantic Oscillation in decadal temperature trends. *Environmental Research Letters*, *12*(11), 114010. https://doi.org/10.1088/1748-9326/aa9152

Kettleborough, J. A., Booth, B. B. B., Stott, P. A., & Allen, M. R. (2007). Estimates of uncertainty in predictions of global mean surface temperature. *Journal of Climate*, *20*(5), 843–855. https://doi.org/10.1175/JCLI4012.1

Knutti, R., Allen, M. R., Friedlingstein, P., Gregory, J. M., Hegerl, G. C., Meehl, G. A., et al. (2008). A review of uncertainties in global temperature projections over the twenty-first century. *Journal of Climate*, *21*(11), 2651–2663. https://doi.org/10.1175/2007JCLI2119.1

Lee, J.-Y., Marotzke, J., Bala, G., Cao, L., Corti, S., Dunne, J., et al. (2021). Future global climate: Scenario-based projections and near-term information. In V. Masson-Delmotte, P. Zhai, A. Pirani, S. L. Connors, C. Péan, S. Berger, et al. (Eds.), *Climate Change 2021: The Physical Science Basis. Contribution of Working Group I to the Sixth Assessment Report of the Intergovernmental Panel on Climate Change* (pp. 553–672). Cambridge University Press. https://doi.org/10.1017/9781009157896.006

O'Reilly, C. H., Befort, D. J., Weisheimer, A., Woollings, T., Ballinger, A., & Hegerl, G. (2021). Projections of northern hemisphere extratropical climate underestimate internal variability and associated uncertainty. *Communications Earth & Environment*, *2*, 194. https://doi.org/10.1038/s43247-021-00268-7

Scaife, A. A., & Smith, D. (2018). A signal-to-noise paradox in climate science. *npj Climate and Atmospheric Science*, *1*, 28. https://doi.org/10.1038/s41612-018-0038-4

Schurer, A., Hegerl, G., Ribes, A., Polson, D., Morice, C., & Tett, S. (2018). Estimating the transient climate response from observed warming. *Journal of Climate*, *31*(20), 8645–8663. https://doi.org/10.1175/JCLI-D-17-0717.1

Schurer, A. P., Hegerl, G. C., Goosse, H., Bollasina, M. A., England, M. H., Smith, D. M., & Tett, S. F. B. (2023). Role of multi-decadal variability of the winter North Atlantic Oscillation on Northern Hemisphere climate. *Environmental Research Letters*, *18*(4), 044046. https://doi.org/10.1088/1748-9326/acc477

Shiogama, H., Stone, D., Emori, S., Takahashi, K., Mori, S., Maeda, A., et al. (2016). Predicting future uncertainty constraints on global warming projections. *Scientific Reports*, *6*(1), 18903. https://doi.org/10.1038/srep18903

Smith, D. M., Scaife, A. A., Eade, R., Athanasiadis, P., Bellucci, A., Bethke, I., et al. (2020). North Atlantic climate far more predictable than models imply. *Nature*, *583*(7818), 796–800. https://doi.org/10.1038/s41586-020-2525-0

Stott, P. A., & Kettleborough, J. A. (2002). Origins and estimates of uncertainty in predictions of twenty-first century temperature rise. *Nature*, *416*(6882), 723–726. https://doi.org/10.1038/416723a

Thompson, D. W. J., Wallace, J. M., & Hegerl, G. C. (2000). Annular modes in the extratropical circulation. Part II: Trends. *Journal of Climate*, *13*(5), 1018–1036. https://doi.org/10.1175/1520-0442(2000)013⟨1018:AMITEC⟩2.0.CO;2

Tokarska, K. B., Hegerl, G. C., Schurer, A. P., Forster, P. M., & Marvel, K. (2020). Observational constraints on the effective climate sensitivity from the historical period. *Environmental Research Letters*, *15*(3), 034043. https://doi.org/10.1088/1748-9326/ab738f